Journal of the Korean Nuclear Society
Volume 29, Number 1, pp. 58~67, February 1997

A Numerical Study on Mixing Characteristics of the Chemical Injection Tank

Keun-Sun Chang
Sun Moon University
100 Kalsanri, Tangjeongmyun, Asansi, Chungnam 336-840, Korea

Byeong-Ho Park
Korea Power Engineering Company, Inc.
150 Dukjin-dong, Yusong-gu, Taejon 305-353, Korea

(Received June 4, 1996)

Abstract

A numerical study has been performed to investigate the flow and mixing characteristics of a chemical injection tank in the chemical and volume control system (CVCS) of Yonggwang 5&6 (YGN 5&6). This study was undertaken to provide a basis for modification of the previous design (YGN 3&4) which gave a lot of difficulties in installation and operation of the chemical injection system during the start-up test because it needs a special reciprocating pump with a high actual head. For the tank of length-to-diameter ratios (L/D) of 1, 2 and 3, each with and without a baffle inside, calculation results were obtained by solving the unsteady laminar two-dimensional elliptic forms of governing equations for the mass, momentum and species concentration. Finite-difference method was used to obtain discretized equations, and the SIMPLER solution algorithm, which was developed based on the staggered grid control volume, was employed for the calculation procedure. Results showed that the baffle is very effective in enhancing the mixing in the tank, and that a baffle should be installed near the tank entrance in order to inject chemicals into the reactor coolant system (RCS) within the operating time required.

1. Introduction

In PWR plants, the reactor coolant system (RCS) must contain an amount of chemicals during the normal operation to prevent material corrosions caused by various impurities such as dissolved oxygen, oxidizing species and chloride[1]. Most of activated corrosion products and fission products are deposited on the low velocity area or out-of-core surface of the reactor pressure vessel. These radioactive nuclides are then transferred into the RCS through the primary coolant. The nuclides are major sources of radiation exposure for plant operation and maintenance personnel. Chemistry control of the RCS is therefore also important to reduce the radiation level.

Chemistry control of the primary coolant is performed by the CVCS chemical addition system and volume control tank. The most important function of the water chemistry control is to minimize the dissolved oxygen concentration and maintain pH within the desired range. Dissolved oxygen is the primary cause of corrosions in the RCS, and the radiation lev

el is strongly dependent on pH in the reactor coolant. The chemical addition system is used for the removal of dissolved oxygen by means of hydrazine injection when the RCS average temperature is below 150°F (65.5℃). Since hydrazine is decomposed into ammonia at higher temperatures, the volume control tank is used to control the dissolved oxygen concentration by injecting hydrogen into the coolant during normal operation (i. e., the RCS average temperature>150°F), in which excessive hydrogen concentration reacts with and removes dissolved oxygen. The concentration of hydrogen in the RCS is controlled by adjusting the hydrogen atmosphere (pressure) in the volume control tank. Normal operational control of the pH is made by maintaining lithium concentration within the design range through the chemical addition system. These chemicals are mixed with reactor makeup water to the desired concentration level in the chemical injection tank of the chemical addition system.

The chemical addition system of YGN 3&4 and UCN 3&4(Ulchin 3&4), which consists of a chemical injection tank, a chemical injection pump and a strainer, is located downstream of the CVCS charging pumps[2]. The system requires a dedicated high pressure positive displacement pump to inject chemicals into the reactor coolant because the system is located on a high pressure piping system (185 kg/cm^2). This type of arrangement has some advantages in that systems and components upstream of the chemical addition system are not contaminated by chemical additives. On the other hand, there is quite a possibility of loss of the system function if the pump fails. Considerable cost effects are also expected for the pump purchase and maintenance. Since YGN 3&4 has experienced a number of technical problems during the start-up test in the installation and operation of the pump, necessity of a design improvement has been recognized.

In this study, a design modification is proposed such that the chemical addition system is to be moved from a downstream to an upstream location of the CVCS charging pumps. This modification makes it possible to use the existing reactor makeup pump for the chemical injection function also, since the system can be operated under the low pressure condition (2.8~4.9 kg/cm^2). The previously used chemical injection pump is eliminated. The modification requires an analysis of mixing characteristics in the chemical injection tank to predict design parameters such as the operating time and the geometrical parameters of the tank.

In many investigations in the past[3,4,5], the characteristics of fluid mixing in a vessel have been identified for the stirred tank. It is clear that, in this case of active means, mixing increases rapidly with one or more impellers installed in the tank. Selection of agitation systems for stirred vessels is both a complex and a difficult task. However, the most reliable information about the mixing process is often given by actual measurement[6,7]. An experimental investigation involving full-scale equipment can be used to predict how identical copies of the equipment would perform under the same conditions. Such full-scale tests are, in most cases, prohibitively expensive and often impossible.

Yoo and So[8] investigated variable density effects on the axisymmetric sudden-expansion flow and indicated that the flow was largely influenced by the inlet Reynolds number and geometric parameters. Much research[9,10,11] has been performed on the characteristics of mass transfer rates in separated aqueous flows for geometries similar to the study of Yoo and So. These investigations all revealed that mass transfer in complex geometries is strongly dependent on local hydrodynamic conditions, and corrosion in aqueous solution is mass transfer controlled. However, as far as the authors are concerned, previous studies similar to the specific flow geometry under consideration have not been found so far.

In this study, a numerical analysis is performed to investigate the flow and mixing characteristics of the chemical injection tank. In order to determine the

optimum aspect ratio (L/D) of the tank, case studies are performed for various injection velocities (i. e., various inlet pipe diameters) and tank aspect ratios with the fixed tank volume and inlet flow rate, each with and without a baffle inside the tank. The tank volume and the injection flow rate are $4.16\times10^{-2}m^3$ and $1.26\times10^{-4}m^3/s$, respectively. Calculation results are obtained by solving the unsteady two-dimensional conservation equations for the mass, momentum and species. Finite-difference procedure is employed for the calculation procedure, and solutions are obtained iteratively using the SIMPLER(Semi-Implicit Method for Pressure Linked Equations Revised) algorithm.

2. Mathematical and Physical Model

2.1. Governing Equations

The capacity of the chemical injection tank is determined based upon the maximum anticipated amount of chemicals to be added in one batch. In the present study, mass transfer in water flow through the injection tank is modeled by a control volume method. The calculation domain is selected to analyze the mixing characteristics in the tank, as shown in Fig. 1. The flow is symmetric with respect to the plane passing through the center of the tank. Therefore, the solution domain is the half of the cylindrical tank, bounded by the symmetry axis and walls.

The concentration and the velocity components obey the general differential governing equations. The major assumptions made for the solution of the governing equations are as follows;

(a) The flow is unsteady two-dimensional laminar flow.
(b) The fluid is incompressible, and thus the variation of fluid properties due to compressibility is neglected.
(c) The temperature in the tank is constant, and natural convection and viscous dissipation effects are neglected.

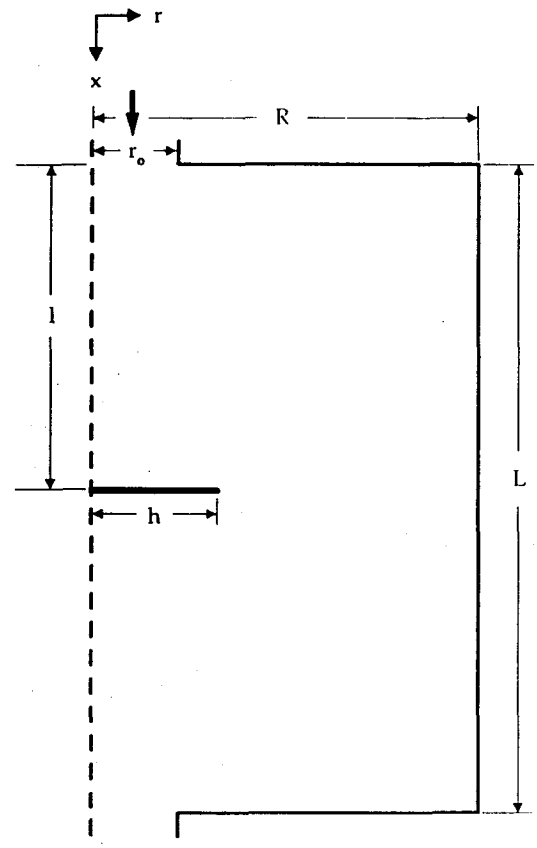

Fig. 1. Schematic of the Physical Model

(d) There are no chemical reactions.

A solution is sought for a set of elliptical partial differential transport equations that all have the same form in the cylindrical coordinate as

$$\rho\frac{\partial\Phi}{\partial t}+\frac{\partial}{\partial x}(\rho U\Phi)+\frac{1}{r}\frac{\partial}{\partial r}(r\rho V\Phi)$$

$$=\frac{\partial}{\partial x}(\Gamma_\Phi\frac{\partial\Phi}{\partial x})+\frac{1}{r}\frac{\partial}{\partial r}(r\Gamma_\Phi\frac{\partial\Phi}{\partial r})+S_\Phi \quad (1)$$

where Φ is the general dependent variable such as U, V, C, and Γ_Φ is the general form of diffusion coefficients, for example, μ in momentum equations, and S is the source term which includes all terms except the convection and diffusion terms. The quantities, Γ_Φ and S_Φ are specific to a particular dependent variable of Φ. The definition of Γ_Φ and S_Φ is presented in Table 1.

Table 1. Definition of Φ, Γ_Φ and S_Φ for the General Governing Equations

Conserved Property	Φ	Γ_Φ	S_Φ
Mass	1	0	0
x-Momentum	U	μ	$\rho g - \frac{\partial P}{\partial x}$
r-Momentum	V	μ	$-2\mu\frac{V}{r^2} - \frac{\partial P}{\partial r}$
Concentration	C	ρD_{AB}	0

2.2. Initial and Boundary Conditions

Since the set of partial differential flow equation, Eq. (1) is parabolic in time and elliptic in space, it is necessary to define initial and boundary conditions for all variables on all boundaries of the flow domain, i. e., inlet, outlet, walls and symmetry axis. At the inlet, all dependent variables are prescribed as given by design values, while zero gradients of all of the dependent variables in the x direction can be set at the outlet (a fully developed condition). In the actual calculation process, the outlet was extended further downstream to make the fully developed condition appropriate. At the symmetry axis, the normal gradients of all dependent variables except the normal velocity component are set to zero and the normal velocity is taken to be zero (V=0). The boundary conditions of the problem are associated with no-slip, impermeable walls. Therefore, no-slip boundary conditions are given to velocity components and zero gradient conditions for the species concentration at the walls (Neumann condition). When the velocity equations are solved, the velocities at the baffle located inside the solution domain can be set to zero by the use of a very large viscosity (for example, 10^{30} kg/m·sec) at the grid points in that region. The infinite value of viscosity results in infinite diffusion, and thus velocities become successively zero from zero velocity at the outer boundary in the computation process. The initial and boundary conditions are summarized in Table 2.

Table 2. Initial and Boundary Conditions

		U(m/s)	V(m/s)	C(kg/kg)
Initial Conditions		0	0	C_0
B. C.	Inlet	U_I	0	C_I
	Symmetry	$\frac{\partial U}{\partial r}=0$	0	$\frac{\partial C}{\partial r}=0$
	Outlet	$\frac{\partial U}{\partial x}=0$	$\frac{\partial V}{\partial x}=0$	$\frac{\partial C}{\partial x}=0$
	Baffle	0	0	0
	Side Wall	0	0	$\frac{\partial C}{\partial r}=0$
	Top & Bottom Walls	0	0	$\frac{\partial C}{\partial x}=0$

2.3. Numerical Scheme

The governing equations were discretized using the finite-difference method on meshes of orthogonally intersecting grid lines. This framework is the control volume approach developed by Patankar[12]. Staggered grids are employed in this approach for the velocity components to avoid wavy field of pressure distribution. The discretized equations were solved iteratively by line-by-line procedure of the tri-diagonal matrix, and the velocity-pressure link through the continuity equation is made by the SIMPLER algorithm[13].

Grid nodes were densely distributed along the boundaries (i. e., inlet, outlet, walls, symmetry axis and baffle boundaries) of the computational domain where steep variations are predicted to occur initially. Preliminary experiments and trial runs were conducted, and the resulting information was used to decide the number of grids for the final experiment. The grid distribution in the x and r direction is 50 and 30.

In order to improve convergence, under-relaxation factors were used both for the velocity components and species concentration. The optimum values of under-relaxation factors depend upon the nature of the problem, the number of grid points and the grid spacing. These values were found from exploratory

computations. Typical values used were from 0.2 to 0.5 for the velocity components and 0.7 to 1.0 for the species concentration. The converged solutions at each time step were assumed to be obtained when relative errors of all variables between two successive iterations are less than 10^{-6}. The first time step was taken to be small (i. e., $\Delta t = 1$ sec), while every subsequent interval was proportionally increased by 10% over the previous one. At the initial time steps, approximately 500 iterations were required to obtain converged solutions at each time step, and the iterations were significantly reduced with lapse of time, and when approaching steady state solutions, only 7~8 iterations were enough to obtain converged solutions. The time required for the steady state solutions of the velocity field depends on the under-relaxation factors used, presence of baffle and inlet velocity. Typical time required for the steady state solutions for the velocity field without baffle is tabulated in Table 3. With the baffle, the time required for the steady state solutions was approximately 40 sec for $L/D = 2$ and $U_i = 0.226$ m/s (15 sec longer than the case without baffle). Definition of the steady state condition for species concentration may be arbitrary because complete dilution ($C = 0$) of fluid initially contained in the tank can not be obtained numerically. In this study, the condition was assumed to be achieved when the concentration drops below 0.1%. The steady state condition for the concentration field could not be achieved without baffle up to 2 hour operation, but with the baffle the condition was reached between 1/2 to 1 hour operation, which varies with the location of the baffle.

3. Results and Discussion

Case studies were performed to determine the optimum geometry of the tank for the fixed tank volume and inlet flow rate given in design requirements. The tank aspect ratios (L/D) investigated are 1, 2 and 3, and inlet velocities are 0.226 m/s and 0.643 m/s for each aspect ratio. The geometric and dynamic parameters of the flows are given in Table 3.

With the baffle, a case is selected for detailed analysis for the tank with $L/D = 2$ and $U_i = 0.226$ m/s. In this case, primary interest is given to the effects of baffle location on the mixing characteristics. The baffle locations are chosen to be $l/L = 1/6$, 3/6 and 5/6 for the same ratio of the baffle radius to tank radius, $h/R = 1/3$.

Fig. 2 shows the calculated results of the time varing average concentration profiles of liquid initially in the tank for each test case without baffle. The average concentration in the tank decreases almost proportionally with time in all test cases. As shown in this figure, more than 30% of the chemicals remains in the tank up to 2 hour injection operation, and mixing is more effective at lower inlet velocities and larger aspect ratios. The flow from the inlet pipe into the much larger tank diameter behaves like a free jet through the quiescent ambient fluid. The flow is convective downstream and diffuses out before impinging the downstream wall. Diffusive force is more pronounced than convection force when the inlet vel-

Table 3. Geometric, Dynamic Parameters and Stability Time of Velocity Field Without Baffle

U_i(m/s)	Inlet Diameter d(m)	Tank Length L(m)	Tank Diameter D(m)	L/D	Stability Time of Velocity Field(sec)
0.226	0.0266	0.376	0.376	1	35
		0.600	0.300	2	25
		0.786	0.262	3	15
0.643	0.0158	0.376	0.376	1	85
		0.600	0.300	2	55
		0.786	0.262	3	35

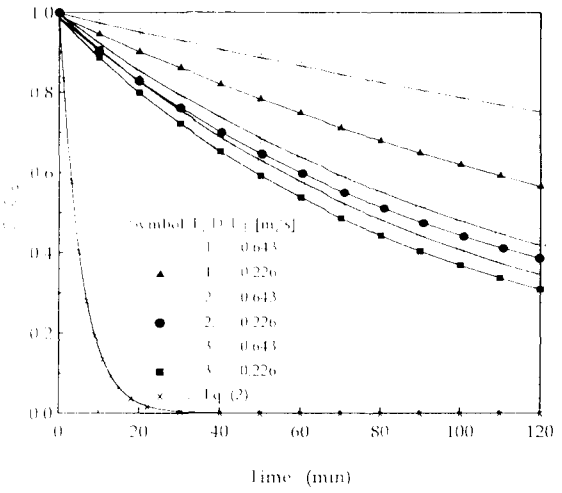

Fig. 2. Time Dependent Average Concentration for Various Tank Geometries and Inlet Velocities Without Baffle

ocity is lowered. For the larger aspect ratio (smaller tank diameter), the mixing region of the free jet type flow becomes larger relative to the unaffected region of the tank, and the side wall effects on the mixing would be more significant.

The feed and bleed method has been often employed to inject the chemicals into the primary coolant of the PWR. The feed and bleed equation [14] can be used to evaluate the time-dependent variation of the mass concentration in the chemical injection tank, which is

$$C = C_{IN} + (C_0 - C_{IN})\exp\left(-\frac{W_{IN}}{W_{TANK}}t\right) \qquad (2)$$

where t = time, (sec)

C_{IN} = mass concentration of chemicals in inlet fluid, (kg/kg)

C_0 = initial mass concentration in tank, (kg/kg)

W_{IN} = mass flow rate of inlet fluid, (kg/s)

W_{TANK} = mass of fluid in tank, (kg)

The calculated results of this study are compared to the values obtained using the theoretical mixing equation(Eq. (2)). Fig. 2 shows that significant differences exist between the results of six numerical experiments of this study and the predicted result obtained by the perfect mixing expressed in Eq. (2). It can be inferred from this result that the desired mixing may not be achieved within the given operating time by only varing the tank geometry or inlet velocity.

Fig. 3 shows streamlines at various time steps for the tank of L/D=2 and U_I=0.226m/s without baffle. The result shown in Fig. 3(d) is the streamlines at the steady state of the velocity field. The behaviors of streamlines at the steady state of other test cases without baffle, which are not shown in this paper, are very similar to those of Fig. 3(d).

From Fig. 3, it can be seen that most of the fluids pass along the symmetry axis by forming weak recirculation in the outer region. At t=2 sec, the inlet fluid is confined in upstream region, causing the weak reverse recirculation in the left upper region where the pressure is relatively low. At this time step, the convective force of the inlet fluid pushes out the front fluid, which initiates the large slow movement

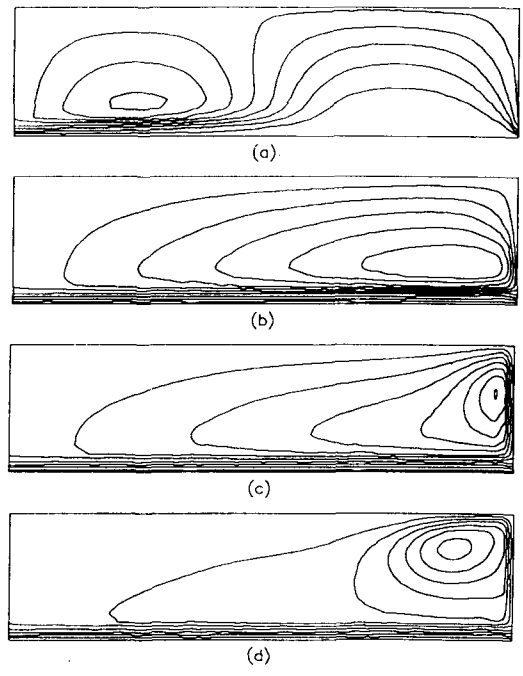

Fig. 3. Profiles of Streamlines without Baffle for L/D=2 and U_I=0.226m/s : (a) 2sec ; (b) 6sec ; (c) 10sec ; (d) 60sec

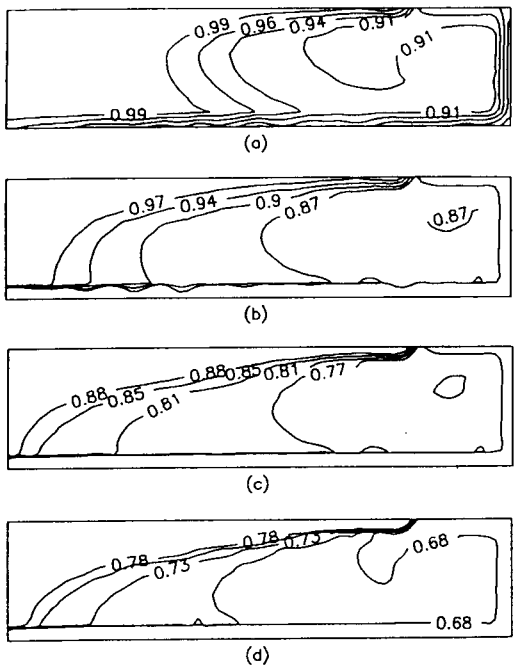

Fig. 4. Profiles of Concentration Isocontours without Baffle for L/D=2 and U_i=0.226m/s : (a) 300sec ; (b) 600sec ; (c) 1200sec ; (d) 1800sec

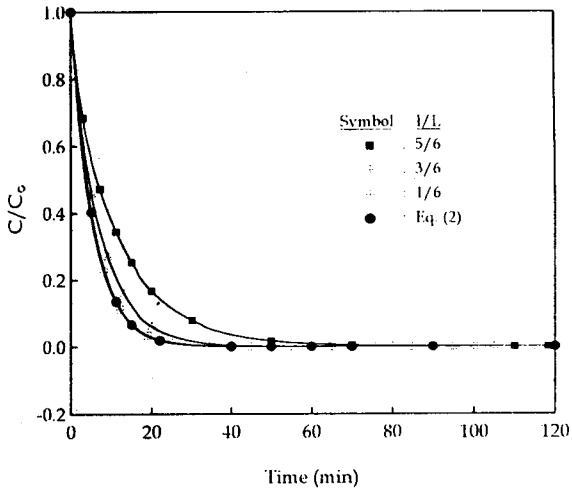

Fig. 5. Time Dependent Average Concentration for Various Baffle Positions for L/D=2 and U_i= 0.226m/s

of the initially stationary fluid. As time passes, the inlet fluid reaches the exit boundary plane and the mixed fluids pass through the exit. The recirculation develops downstream with time into the entire outer region, but with the strength being increased and the center moved downstream, which in turn results in effective mixing at near the exit boundary. Fig. 4 reflects this more clearly. Fig. 4 presents profiles of iso-concentration contours for the tank of the same aspect ratio and inlet velocity as those of Fig. 3, but for different time steps (t=300, 600, 1200 and 1800 sec). High concentration fluid (i. e., fluid initially in the tank) is trapped in the left upper coner of the tank, which is characterized by very weak recirculation fluid in that region as discussed previously. The concentration decreases downstream as the relatively stronger recirculation develops downstream with time.

Effect of the baffle on the mixing has been investigated for the selected tank geometry with L/D=2, and U_i=0.226 m/s. Three different baffle locations (l/L=1/6, 3/6 and 5/6) as shown in Fig. 1 are investigated. The baffle height is fixed as h/R=1/3 in all cases. Fig. 5 shows the time varing average concentration in the tank of three test cases with the baffle. It can be seen that, compared to profiles without baffle (Fig. 2 for L/D=2, U_i=0.226 m/s), the intensity of mixing is significantly increased for all cases with the baffle, and effective mixing occurs at initial period of time (at t=60 min, C/Co less than 0.01 with the baffle, but approximately 0.6 without the baffle). Fig. 5 also shows that the mixing is more effective when the baffle is installed closer to the entrance at initial period of time (l/L=1/6). This is resulted from the stronger recirculation flow created at the region bounded by the walls and baffle when the baffle location is close to the entrance. This is more evidently seen from the streamline profiles shown in Fig. 6 and the iso-concentration contours in Fig. 7, Fig. 6 and Fig. 7 fairly well show somewhat different mixing mechanism with the baffle (compare to Fig. 3 and Fig. 4 without baffle). As can be seen in Fig. 5, at t>60 min, average concentration profiles in all test cases approach to the zero value, which indicates that the

chemicals initially in the tank are almost completely depleted at that time.

Predicted average concentration is also compared to the theoretical mixing curve of Eq. (2) (Fig. 5). Note that Eq. (2) assumes a perfect mixing at each time step between the injected fluid and the fluid in the tank. Predicted average concentrations with time are comparable to the theoretical mixing curve. Especially for the baffle at $l/L = 1/6$, prediction results of this study show nearly the same mixing profile as that of the theoretical mixing curve obtained using Eq. (2). These results indicate that, for the given tank geometry and flow condition, nearly perfect mixing can be achieved when the baffle is installed closer to the entrance.

4. Conclusions

A numerical study has been performed for the flow in the cylindrical shape of the chemical injection tank to investigate the mixing characteristics and to determine the optimum geometry of the tank for the design application. The calculation results were obtained by solving the unsteady laminar two-dimensional elliptic forms of governing equations for the mass, momentum and species concentration. Finite-difference method was employed for the calculation procedure, together with the SIMPLER solution algorithm which was developed based on the staggered grid control volume. In order to obtain the optimum geometry of the tank, case studies were performed for various inlet velocities (i. e., various inlet line sizes) and tank aspect ratios with and without a baffle.

Results showed that without baffle the average concentration of chemicals in the tank decreases almost proportionally with time in all test cases, and that the mixing is more effective at lower inlet velocities and larger aspect ratios. However, the desired mixing could not be obtained within the operating time req-

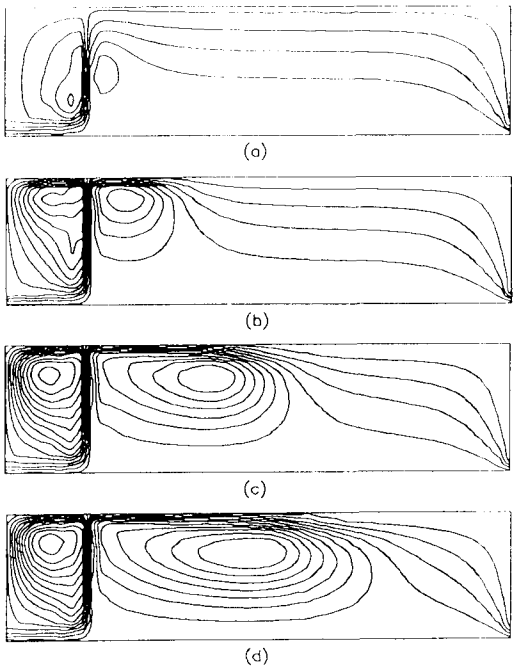

Fig. 6. Profiles of Streamlines with Baffle at $l/L=1/6$ for $L/D=2$ and $U_i=0.226$m/s : (a) 2sec; (b) 10sec ; (c) 30sec ; (d) 60sec

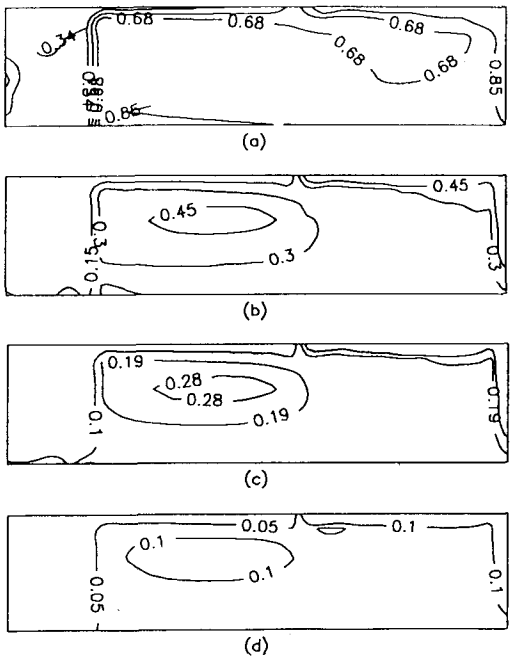

Fig. 7. Profiles of Concentration Isocontours with Baffle at $l/L=1/6$ for $L/D=2$ and $U_i=0.226$m/s : (a) 120sec ; (b) 420sec ; (c) 600sec ; (d) 900sec

uired without baffle. When the baffle is installed, the mixing in the tank is significantly increased compared to the case without baffle. The increasing mixing effect is more pronounced when the baffle is located closer to the tank entrance. Though the desired mixing could be achived in all test cases with the baffle within the operating time required, it was determined that the tank with the baffle at l/L = 1/6, aspect ratio of L/D = 2 and inlet diameter of 0.0266m (i. e., 0.226m/s inlet velocity) was the best one in tank geometry for the design application.

Nomenclature

- C species concentration, kg/kg
- C_I species concentration of injection fluid, kg/kg
- C_O initial species concentration of fluid in the injection tank, kg/kg
- D chemical injection tank diameter, m
- D_{AB} mass diffusivity, m/sec^2
- d inlet diameter, m
- g gravitational acceleration, m^2/sec
- h baffle height, m
- l distance between baffle and tank entrance, m
- L chemical injection tank length, m
- P pressure, N/m^2
- r radial coordinate, m
- r_o inlet and outlet pipe radius, m
- R chemical injection tank radius, m
- S_Φ source term expressed in Eq. (1)
- Sc Schmidt number ($Sc = \frac{\mu}{\rho D_{AB}}$)
- t time, sec
- U,V components of velocity vector, m/sec
- U_I velocity of injection fluid, m/sec
- x axial coordinate, m
- Γ_Φ general diffusion coefficient expressed in Eq. (1), kg/m · sec
- μ viscosity, kg/m · sec
- ρ fluid density, kg/m^3
- Φ general dependent variable expressed in Eq. (1)

References

1. YGN3&4 Nuclear Steam Supply System Chemistry Manual, CENPD-280, ABB-CE/KAERI, (1994)
2. System Description for Chemical and Volume Control System for YGN3&4, 10487-FS-SD410, ABB-CE/KAERI, (1989)
3. Rao, D.P., and L.L. Edwards, "Mixing Effects in Stirred-Tank Reactors : a Comparison of Models", *Chem. Eng. Sci.*, **28**, 1179-1192 (1973)
4. Bouwmans and H.E.A. van den Akker, "The Influence of Viscosity and Density Differences on Mixing Times in Stirred Vessels", *I. Chem. E. Symposium* **121**, 1-12 (1990)
5. Güray Tosun, "A Mathematical Model of Mixing and Polymerization in a Semibatch Stirred-Tank Reactor", *AIChE Journal* **38**, 425-437 (1992)
6. M. Liu, R.L. Peskin, F.J. Muzzio, and C.W. Leong, "Structure of the Stretching Field in Chaotic Cavity Flows", *AIChE Journal* **40**, 1273-1286 (1994)
7. H.M. van Sonsbeek, P. Verlaan, and J. Tramper, "Hydrodynamics, Mixing and Oxygen Transfer in Liquid-Impelled Loop Reactors", *I. Chem. E. Symposium* **121**, 259-268 (1990)
8. G.J. Yoo and R.M.C. So, "Variable Density Effects on Axisymmetric Sudden-Expansion Flows", *Int. J. Heat Mass Transfer* **32**, 105-120 (1989)
9. S. Nešić, J. Postlethwaite and D.J. Bergstrom, "Calculation of Wall-Mass Transfer Rates in Separated Aqueous Flow Using a Low Reynolds Number k-ε Model", *Int. J. Heat Mass Transfer* **35**, 1977-1985 (1992)
10. J. Postlethwaite, M.H. Dobbin, and K. Bergevin, "The Role of Oxygen Mass Transfer in the Erosion-Corrosion of Slurry Pipelines", *Corrosion* **42**, 524-521 (1986)
11. B.K. Mahato, S.K. Voora, and L.W. Shemilt, "Steel Pipe Corrosion under Flow Conditions-I ;

An Isothermal Correlation for a Mass Transfer Model", *Corros. Sci* **8**, 173-193 (1968)

12. S.V. Patankar, "A Calculation Procedure for Two Dimensional Elliptical Situations", *Numer. Heat Transfer* **4**, 409-425 (1981)
13. S.V. Patankar, *Numerical Heat Transfer and Fluid Flow*, McGraw-Hill, New York (1980)
14. R.B. Bird, W.E. Stewart, and E.N. Lightfoot, *Transport Phenomena*, Wiley, New York (1960)